scientific reports

Check for updates

OPEN

Paxilline derived from an endophytic fungus of *Baphicacanthus cusia* alleviates hepatocellular carcinoma through autophagy-mediated apoptosis

Yin Yuan[1,2,6], Jing Yu[1,2,6], Meng Li[3], Tian Zhou[4,5], Zhaoyou Deng[1,2], Cuiyun Yin[1,2], Xuanchao Shi[1,2], Deying Tang[1,2], Yiran Liu[4] & Yihang Li[1,2]✉

Hepatocellular carcinoma (HCC) is a malignancy for which no effective drugs are available. Paxilline is derived from an endophytic fungus of the leaves of *Baphicacanthus cusia* (Nees) Bremek. In a previous study, we found that paxilline inhibited the proliferation of HepG2 cells; however, its mechanism remains unclear. In this study, ESI$^+$ and NMR were used to characterize the paxilline structure. Network pharmacology analysis was performed with databases and software to obtain the core targets and signaling pathways associated with the anti-HCC effects of paxilline. Molecular docking was performed to validate the preliminary affinity of paxilline for the core targets. For further in vitro experiments, a CCK8 assay was performed to detect cell viability, a wound healing assay was performed to detect cell migration, an Annexin V-FITC assay was performed to detect the cell cycle and apoptosis rate in HepG2 cells, RT-qPCR analysis was performed to detect the expression of cell cycle-related genes and autophagy-related genes, Immunofluorescence staining was performed to detect the expression of LC3B, and Western blotting was performed to detect the expression of apoptosis-related proteins and autophagy-related proteins. As a result, we obtained a white powder, which was identified as paxilline. Network analysis and molecular docking results revealed that apoptosis-related and autophagy-relatted protein were key targets (mTOR and PI3K) for paxilline anti-HCC. Further examination revealed that paxilline promoted HepG2 cell apoptosis, inhibited HepG2 cell migration, and arrested HepG2 cell in the S phage. RT-qPCR analysis revealed that paxilline markedly downregulated the mRNA expression of Cyclin D1, CDK4, LC3B, mTOR, Parkin, and PINK1. Immunofluorescence staining demonstrated a significant upregulation of LC3B protein expression following paxilline treatment. Further validation by Western blotting showed that paxilline significantly increased the expression of LC3B II/I, bax, cleaved-PARP, and cleaved-caspase 3, while significantly decreased the expression of bcl-2. Additionally, a significant promotion of cellular apoptosis and expression of apoptotic proteins when treatment with chloroquine (CQ)/rapamycin (Rapa). Meanwhile, when combined with paxilline, it was found that paxilline may have a synergistic effects with Rapa, jointly promoting cellular apoptosis and the expression of proapoptotic proteins. In conclusion, these findings reveled paxilline alleviates HCC through autophagy-mediated apoptosis.

Keywords Paxilline, Hepatocellular carcinoma, Network pharmacology, Apoptosis, Autophagy

Hepatocellular carcinoma (HCC) is a highly prevalent malignant tumor, and the number of deaths due to HCC is the second-highest in China[1,2]. While surgical treatments such as hepatectomy, liver transplantation,

[1]Yunnan Branch, Institute of Medicinal Plant Development, Chinese Academy of Medical Sciences and Peking Union Medical College, Xishuangbanna Dai Autonomous Prefecture 666100, China. [2]Yunnan Key Laboratory of Southern Medicine Utilization, Xishuangbanna Dai Autonomous Prefecture 666100, China. [3]College of Pharmacy, Yunnan University of Chinese Medicine, Kunming 650500, China. [4]Heilongjiang University of Chinese Medicine, Harbin 150040, China. [5]Xishuangbanna Jianlong Pharmaceutical Co., Ltd., Xishuangbanna Dai Autonomous Prefecture 666100, China. [6]Yin Yuan and Jing Yu have contributed equally to this work. ✉email: 48466685@qq.com

and transarterial chemoembolization are the primary means of treating HCC, strict surgical indications and contraindications limit the number of patients who can receive these treatments, and the overall prognosis is poor[3,4]. Although new anticancer drugs for HCC have been developed, the overall prognosis is unsatisfactory. Hence, new drugs need to be developed to improve patient outcomes and their quality of life.

Baphicacanthus cusia (Nees) Bremek, a traditional Chinese medicine, has a wide range of pharmacological activities, such as anti-inflammatory, antibacterial, antitumor, antiviral, and immune-promoting effects, and can protect the liver[5,6]. Paxilline, a secondary metabolite extracted from an endophytic fungus of the leaves of *B. cusia* (Nees), was identified in our previous study[7]. We found that paxilline inhibits the proliferation of HepG2 cells, but its mechanism of action remains unclear.

Autophagy has positive and negative effects on cancer, depending on the environment, leading to cancer cell survival or apoptosis[8,9]. Under stress, autophagy starts with segregating part of the cytoplasm into autophagosomes, which have a double-layered membrane structure that can be detected by converting microtubule-associated protein-1 light chain-3 (LC3 I), to its lipidated form, known as LC3 II. Next, autophagosomes merge with lysosomes, leading to the degradation of damaged cytoplasmic proteins and organelles[10]. Autophagy may be required for the progression of benign tumors to malignant tumors during late tumor progression. HCC develops when the hepatic Atg gene is knocked out in mice[11,12]. Autophagy also occurs concurrently with apoptosis or precedes it. When chemotherapeutic agents are used alone or in combination with chloroquine (CQ, an inhibitor of autophagy) or rapamycin (Rapa, an autophagy agonist) they significantly promote the apoptosis of tumor cells and inhibit tumor growth[13].

Although our study found that paxilline is promising for treating HCC, the mechanisms by which paxilline affect HCC remain unclear. In this study, we investigated whether paxilline induced the apoptosis of HepG2 cells and whether this apoptosis was associated with autophagy. This study provided a theoretical basis for considering paxilline in clinical trials.

Materials and methods

Paxilline isolation

Paxilline was provided by Jing Yu and the detailed extraction methods are described in another study[7]. To summarize, the *Penicillium* sp. Nb 19 fungal strain was extracted from the leaves of *B. cusia* (wfo link: wfo-0000559898), and the medium was supplemented with the *Penicillium* sp. Nb 19 fungal strain was fermented for 30 days at room temperature. The fermentation broth was first extracted by ultrasonication, followed by extraction with petroleum ether, ethyl acetate, and methanol three times. Finally, a rotary evaporator was used to dry the crude extract under a vacuum. The crude extract was mixed with 100–200 mesh silica gel and fractionated by column chromatography. The eluents were different mixtures of dichloromethane-methanol (100:1 to 2:1) for column fractionation, which yielded nine first-order fractions (Fr.1–Fr.9). Fraction 4 was purified and eluted twice through the column to obtain paxilline.

Characterization of paxilline

High-resolution electrospray ionization mass spectrometry (HRESIMS) analyses were performed using an Agilent Accurate-Mass TOF LC/MS 6230 instrument in the positive ion mode (Agilent, USA), and the ion peak m/z was detected. NMR (1H-NMR, 13C-NMR) was performed to detect the paxilline structure (Bruker Avance-500 spectrometer), and tetramethylsilane was used as the internal standard (Bruker, Germany).

Network pharmacology analysis

The targets of paxilline were identified from the Swiss Target Prediction database. The therapeutic targets for treating HCC were identified by searching the following databases: DisGeNet, OMIM, TTD, and GeneCards, with the keywords "hepatocellular carcinoma". Venny 2.1 was used to obtain paxilline-HCC shared targets. For the above-shared targets, the STRING website was used to construct protein–protein interaction (PPI) networks, which were visualized using Cytoscape 3.9.1. Shared targets were identified using the Metascape website for GO and KEGG enrichment analyses ($P < 0.01$).

Molecular docking

The PubChem database (https://pubchem.ncbi.nlm.nih.gov/) was used to acquire MOL2 files for paxilline. The core targets in humans were screened, selected from the UniProt database (https://www.uniprot.org/), and then downloaded in the PDB format from the RCSB PDB platform (PDB, http://www.rcsb.org). After preprocessing the data, the structures were generated using AutoDock Vina and saved as PDBQT files. Docking simulations were performed using AutoDock Vina to study the affinity of the ligands; an affinity of less than or equal to −7 kJ/mol indicated high binding activity. The docking structures were visualized as illustrations using the PyMOL software.

Cell lines

HepG2 cells were purchased from Wuhan Procell Life Co., Ltd. Dulbecco's modified Eagle medium (DMEM) and fetal bovine serum (FBS) were purchased from Gibco (Carlsbad, CA, USA). The cells were maintained in a humidified atmosphere containing 5% CO_2 at 37 °C. The cell lines were authenticated and were not mycoplasma.

Cell viability assays

To determine the concentration of paxilline used to treat HepG2 cells, the CCK-8 assay was performed. HepG2 cells were incubated with different concentrations of paxilline (0, 10 μg/mL, 20 μg/mL, 40 μg/mL, and 80 μg/mL) to determine the optimum paxilline concentration. After 24 h of incubation, HepG2 cell viability was determined using a CCK-8 Kit (Biomiky, Shanghai, China).

Wound healing assays
HepG2 cells were seeded into 6-well plate; when the cells reached 90% confluence, a wound scratch in each well was gently made by a 200 μL pipette. Then washed the wells once with PBS, and then cells were treated with specific concentrations of paxilline (0, 10, 20, and 40 μg/mL) for 0, 24 h, and 48 h. An inverted fluorescence microscope (OLYMPUS, Japan) was used to capture images. The images were analyzed via Image-J Software (MD, USA).

Cell cycle distribution
After exposing HepG2 cells to different concentrations of paxilline (0, 10, 20, and 40 μg/mL) for 48 h, the cells underwent various treatments. The cells were initially harvested, washed, and subsequently fixed. PI/RNase staining buffer (Beyotime, China) was used to incubate the cells in the dark for 30 min. Flow cytometry (BD Biosciences, USA) was performed to measure the DNA content in each phase. The data were subsequently analyzed using ModFit LT version 5.0.

Flow cytometry analysis of apoptosis
HepG2 cells were challenged with various concentrations of paxilline (0, 10, 20, and 40 μg/mL) for 12 h and then harvested using 0.25% trypsin without EDTA. The cells were washed twice with PBS and then resuspended in a binding buffer. Next, Annexin V-FITC and propidium iodide (Beyotime, Beijing, China) were added to the cells, which were subsequently incubated for 15 min in the dark. Finally, the cells were analyzed by flow cytometry to calculate the percentage of apoptotic cells.

Immunocytochemistry staining
HepG2 cells were challenged with paxilline for 24 h. Then, the HepG2 cells were fixed in 4% polyformaldehyde (PFA) for 15 min and washed thrice with PBS. The sections were subsequently incubated with primary antibodies at 4 °C overnight. The cell nuclei were stained blue with DAPI, and an Olympus fluorescence microscope was used to capture the images.

RT-qPCR
Total RNA was extracted using TRIzol (Invitrogen, USA) following the manufacturer's protocol. Next, cDNA was synthesized using a two-step method using a Takara kit (Japan). The cycle times were normalized to those of β-actin in the same sample. The $2^{-\Delta\Delta CT}$ method was used to analyze the acquired mRNA data. The expression levels of the mRNAs were reported as fold changes vs. the control. β-actin was purchased from Sangon Biotech Co., Ltd. (B661302-0001). The primer sequences used for the analysis are listed in Table S1.

Western blotting
Total protein was extracted using RIPA buffer. In total, 10 μg of protein per sample was loaded onto a 4–20% precast gel and then transferred to a PVDF membrane (Millipore, USA). The membranes were blocked for 30 min at room temperature, washed three times, and then incubated with primary antibodies overnight at 4 °C (Table S2). The following day, the membranes were incubated for 1 h with secondary antibodies (ABclonal; 1:10000). After treatment with enhanced chemiluminescence (ECL) reagents (Beyotime, China), the protein bands were visualized using a gel imaging system (Tanon, China). The gray value was normalized to that of β-actin and quantified using the ImageJ software.

Statistical analysis
All experimental data were presented as the mean ± standard deviation. Statistical analysis was performed, and histograms were generated using GraphPad Prism 9. The differences among groups were determined by one-way analysis of variance (ANOVA). All differences were considered to be statistically significant at $P < 0.05$.

Results
Analysis and identification of paxilline from an endophytic fungus of *Baphicacanthus cusia*
Analysis and identification of paxilline via ESI–MS (positive) yielded quasi-molecular ion peaks at m/z 458$[M+Na]^+$ (Fig. S1A). The molecular formula of the compound was determined to be $C_{27}H_{33}NO_4$, based on the ^{13}C NMR and ^1H NMR data (Fig. S1B, C), and the degree of unsaturation was 12. The chemical formulae of paxilline are shown in Fig. S1D.

Collection of potential targets and PPI network construction
From the flow chart of network pharmacology (Fig. 1A), we identified 100 potential targets of paxilline, 9965 targets of HCC, and 76 drug-disease-shared targets. The 76 potential targets were used for PPI network construction using the STRING database (Fig. 1B). After three outlier nodes were removed, the remaining 73 targets were visualized using Cytoscape 3.9.1 (Fig. 1C). The predicted targets were evaluated using degree centrality (DC) to provide a basis for the subsequent core target screening (Table S3).

GO and KEGG enrichment analysis
The GO and KEGG enrichment analyses of overlapping targets were performed using the Metascape platform. The biological processes associated with the overlapping targets included phosphorylation, the cellular response to organonitrogen compounds, the response to growth factors, etc. The cellular components included the receptor complex, the nuclear cyclin-dependent protein kinase holoenzyme complex, the side of the membrane, etc. The molecular functions included phosphotransferase activity, protein kinase activity, and protein phosphatase binding (Fig. 2A, Table S4). The results of the KEGG enrichment analysis revealed that 'pathways in cancer'

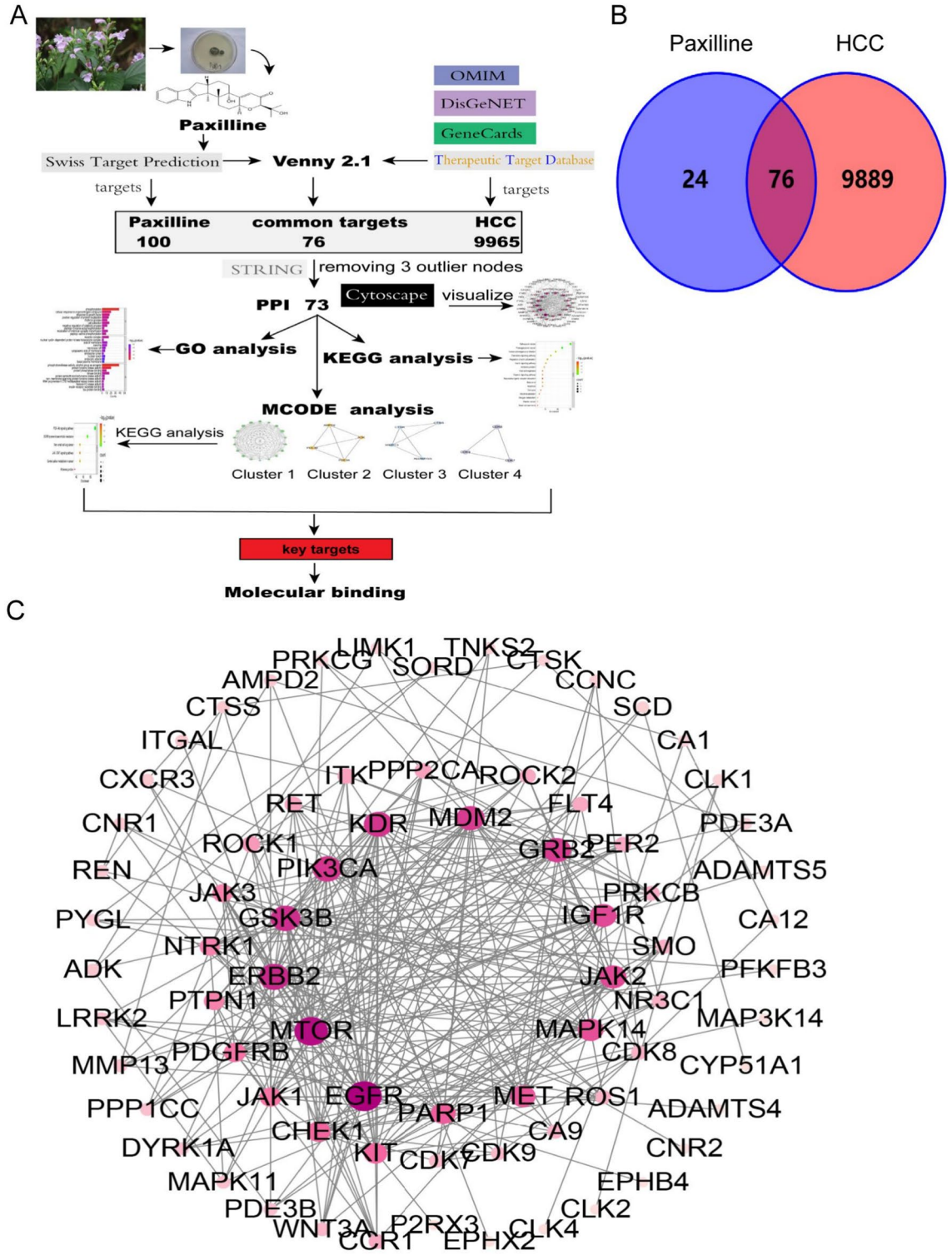

Fig. 1. Network analysis of paxilline for the treatment of HCC. (**A**) Flow chart of network pharmacology. (**B**) Venn diagram of paxilline and HCC targets. (**C**) PPI diagram of the paxilline anti-HCC agent. The more pink and larger the nodes, the greater the contribution of the target to the network.

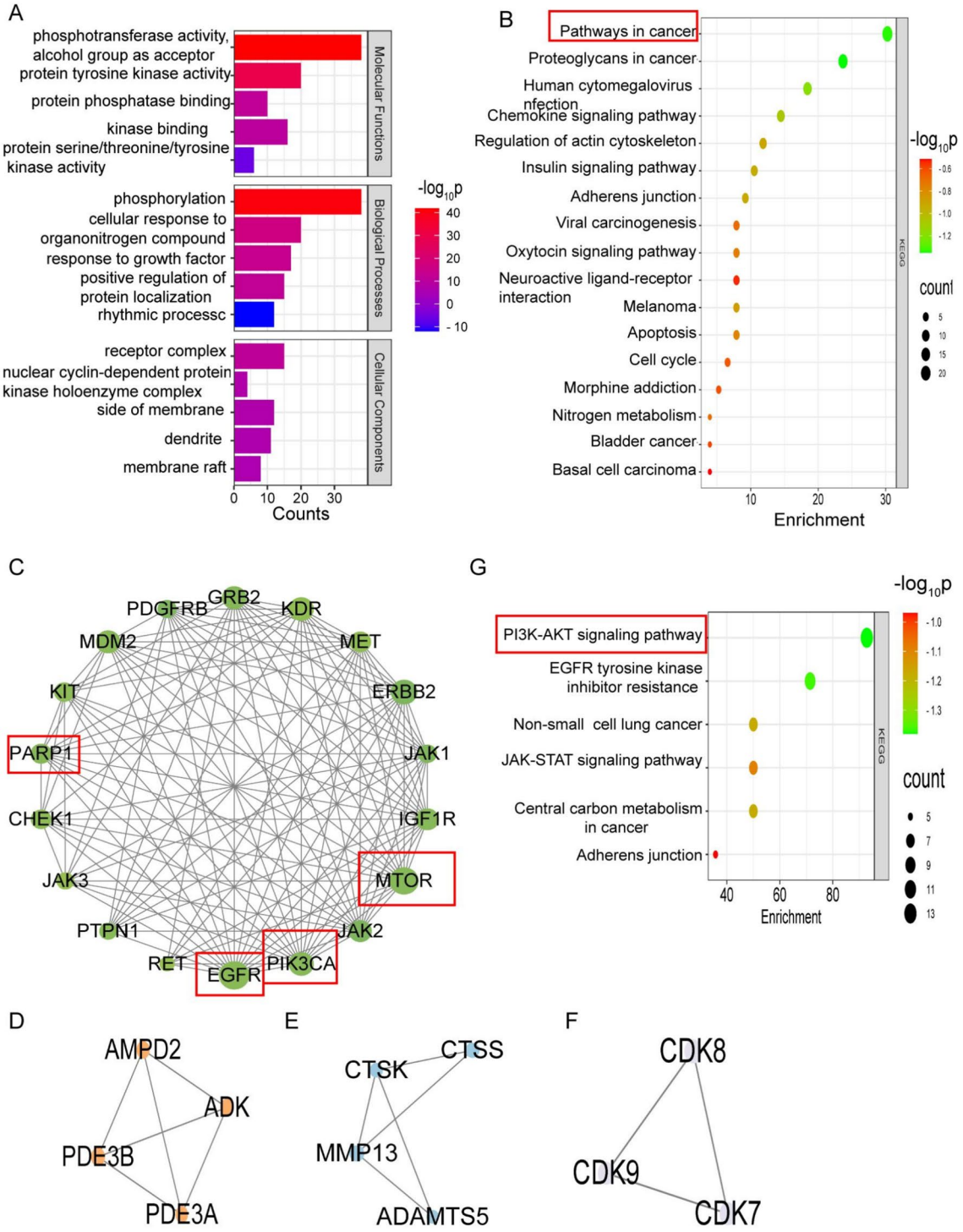

Fig. 2. GO, KEGG, and MCODE analyses. (**A**) GO analysis of the core targets. (**B**) KEGG analysis of the core targets. The greener and greater the number of targets, the greater the significance of the pathways. (**C**–**F**) The core targets were analyzed using the MCODE plugin and clustered according to apoptosis, energy metabolism, extracellular matrix remodeling, and cell cycle clustering. (**G**) Targets from cluster 1-enriched signaling pathways.

was the most important term in the prediction results (Fig. 2B, Table S5). Additionally, "pathways in cancer" is closely related to cell proliferation, growth, differentiation, and apoptosis (Fig. S2).

MCODE analysis

To further elucidate the underlying mechanisms, the MCODE algorithm was used to screen core targets from the PPI network, and four clusters were obtained (Fig. 2C–F). Analysis of the clustered targets revealed that cluster 1 was related mainly to apoptosis, cluster 2 was related mainly to energy metabolism, cluster 3 was related mainly to extracellular matrix remodeling, and cluster 4 was related mainly to the cell cycle. Cluster 1 was found to enrich targets with the highest degree value. Therefore, cluster 1 was the most important result of the MCODE analysis, which showed that EGFR and mTOR were the most crucial targets (Fig. 2C, Table S3) and enriched signaling pathways, including the PI3K-AKT, EGFR tyrosine kinase inhibitor resistance, and non-small cell lung cancer pathways (Fig. 2G).

Molecular docking

To further validate the interactions between paxilline and the identified targets, molecular docking analysis was performed. The targets of mTOR (**PDB ID:** 1FAP), PIK3CA (**PDB ID:** 8EXL), PARP1 (**PDB ID:** 1UK0), and EGFR (**PDB ID:** 8A27) were selected as the docking receptors, and paxilline served as the ligand. These targets were closely related to apoptosis or autophagy. The cartoon showed the binding pockets of paxilline to the target site, whereas the affinity analysis quantified the binding ability between paxilline and its receptors. The absolute value of the affinity was used to measure the binding strength between two molecules. As shown in Fig. 3A, paxilline could bind with core targets and form five hydrogen-bond interactions with mTOR, two hydrogen-bond interactions with PIK3CA, and one hydrogen-bond interaction with PARP1 and EGFR. The results shown in Fig. 3B and Table S6 suggested strong binding between paxilline and both mTOR (affinity = − 8.1) and PIK3CA (affinity = − 9.8).

Paxilline suppresses the proliferation and migration of HepG2 cells

The HepG2 cells were challenged with different concentrations (0, 10, 20, 40, and 80 μg/mL) of paxilline for 24 h (Fig. 4A). The cells in the control group were irregularly shaped; these cells adhered firmly to the wall and grew in clusters, and the connections between the cells were tight. However, the morphology of other groups of cells changed from irregular to rounded. Nonadherent cells appeared in the culture medium, the gap between cells became more extensive, and the change in cell morphology became more apparent. The number of dead cells increased as the dose of paxilline increased. The results of the CCK8 assay suggested that paxilline significantly decreased the viability of HepG2 cells at 40 μg/mL and 80 μg/mL ($P < 0.001$), and the half-maximal inhibitory concentration (IC50) was 48.49 μg/mL (Fig. 4B). Thus, we selected 10, 20, and 40 μg/mL paxilline to evaluate its activity in another experiment. We also assessed the effect of paxilline on HepG2 cell migration by conducting wound-healing assays. Compared to those in the control group, the number of HepG2 cells treated with paxilline was considerably delayed at 24 h in a dose-dependent manner ($P < 0.001$) (Fig. 4C).

Paxilline arrests HepG2 cells in the S phase

After treatment with paxilline for 48 h, the percentage of HepG2 cells in the S phase increased in a dose-dependent manner, whereas the number of G0/G1 phase cells decreased significantly (Fig. 5A). Moreover, paxilline inhibited the expression of cyclin D1 and CDK4 ($P < 0.001$) (Fig. 5B, C).

Paxilline triggers apoptosis in HepG2 cells

By evaluating the cell cycle, we found that paxilline blocked HepG2 cells in the S phase, influencing DNA synthesis. Therefore, in the next experiment, the percentage of apoptotic HepG2 cells was determined after treatment with paxilline. Compared to the control, paxilline significantly promoted HepG2 cell apoptosis (Fig. 6A), which approximately 50–95% with a dose-dependent (Fig. 6B). To determine the effect of paxilline on HepG2 cells, we examined the expression of apoptosis-related proteins. The results suggested that paxilline significantly inhibited the expression of bcl-2 and promoted the expression of bax, cleaved caspase-3, and cleaved-PARP in HepG2 cells (Fig. 6C). These results indicated that paxilline significantly promoted the apoptosis of HepG2 cells.

Paxilline regulates autophagy in HepG2 cells

The results of the network pharmacology analysis revealed that the therapeutic effect of paxilline on HCC may be related to autophagy. Therefore, we analyzed the mRNA expression of genes associated with autophagy by RT-qPCR. These results indicated that paxilline (40 μg/mL) considerably decreased the mRNA expression of mTOR, Parkin, Pink1, and LC3B ($P < 0.001$) (Fig. 7A–D). These results suggested that paxilline may regulate autophagy. LC3s is a critical protein in autophagy and marks the generation of autophagosomes. Thus, we examined the expression of LC3B after different concentrations of paxilline were added to HepG2 cells. The results of the immunofluorescence assays revealed a varying degree of increase in the fluorescence intensity of LC3B after HepG2 cells were treated with different concentrations of paxilline, with the highest expression occurring at 40 μg/mL (Fig. 7E, F). As shown in Fig. 7G, paxilline significantly increased the LC3B-II/LC3B-I ratio in HepG2 cells ($P < 0.05$).

Paxilline promotes apoptosis by regulating autophagy in HepG2 cells

Based on the previous results, we hypothesized that the ability of paxilline to promote the apoptosis of HepG2 cells might be related to autophagy. To test this hypothesis, we examined the apoptosis rate of HepG2 cells and the expression of apoptosis-related proteins using CQ and Rapa. The results of an apoptosis assay revealed that paxilline, CQ, Rapa, paxilline + CQ, and paxilline + Rapa significantly increased the apoptosis rate of HepG2

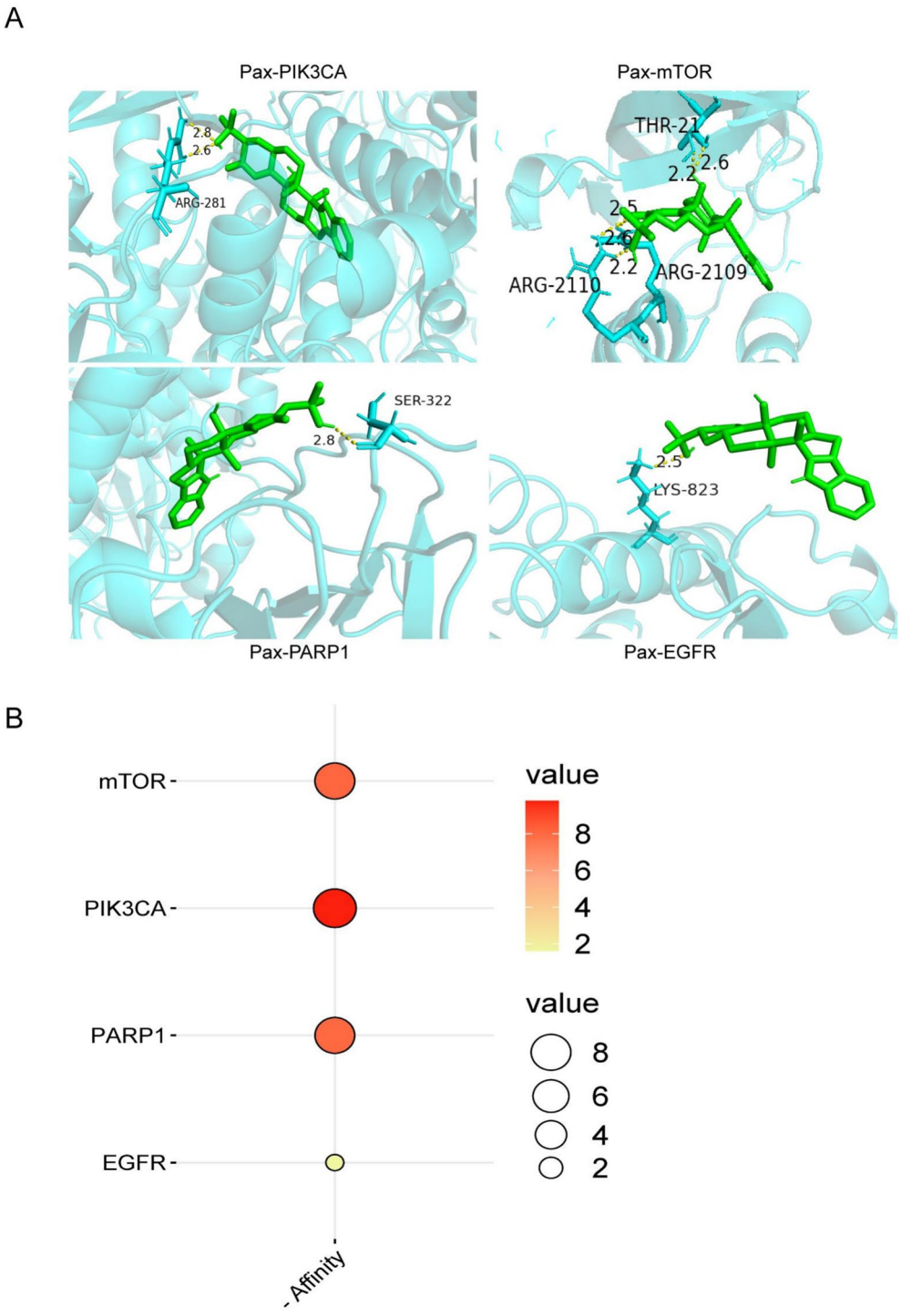

Fig. 3. Molecular docking results showed that paxilline acts on apoptosis-related or autophagy-related targets. (**A**) Docking cartoon between paxilline and core targets. Molecular docking simulations were carried out using AutoDock Tools (version 1.5.7), with subsequent visualization performed in PyMOL (version 2.5.0). (**B**) The affinity between paxilline and core targets was determined. The redder and larger the dots, the greater the absolute value of the affinity.

cells ($P < 0.001$) (Fig. 8A, B). Western blotting analysis revealed that paxilline, CQ, Rapa, paxilline + CQ, and paxilline + Rapa considerably upregulated the expression of LC3BII/I, cleaved-PARP, cleaved caspase-3, and bax and substantially downregulated bcl-2. Further analysis revealed that the expression of LC3BII/I, cleaved-PARP, and bax in the CQ + paxilline group was lower than that in the CQ group ($P < 0.01$). The expression of cleaved-PARP, cleaved caspase-3, and bax in the Rapa + paxilline group was greater than that in the Rapa group ($P < 0.001$) (Fig. 8C).

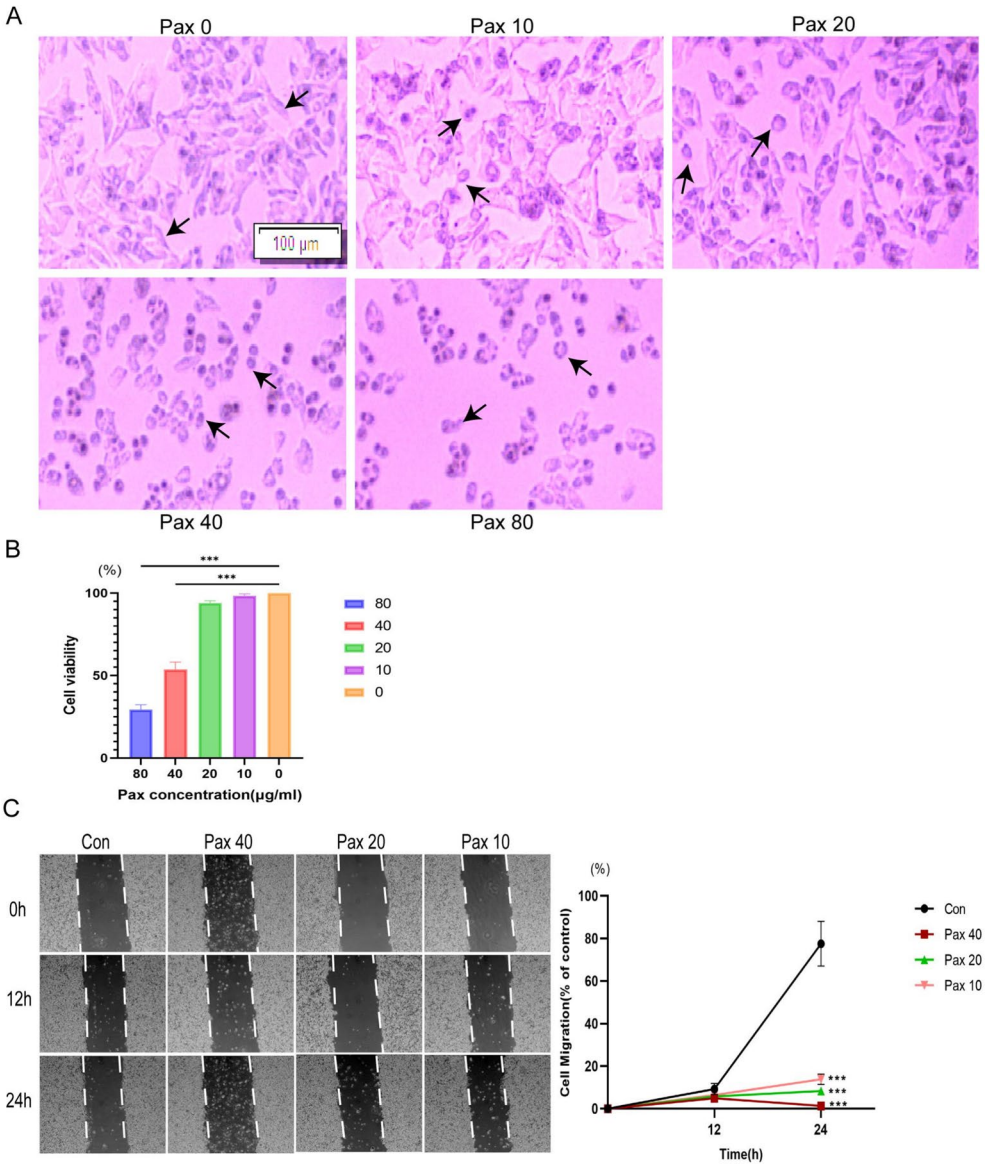

Fig. 4. Screening of the effects of various concentrations of paxilline on HepG2 cells for growth and movement. (**A**) Images of HepG2 cells after treatment with different concentrations of paxilline (0, 10, 20, 40, and 80 μg/mL); scale bar = 100 μm; arrows indicate cell morphology. (**B**) The viability of HepG2 cells after treatment with different concentrations of paxilline (0, 10, 20, 40, and 80 μg/mL) was determined by the CCK8 assay. (**C**) HepG2 cell movement was evaluated by conducting wound-healing assays at 0, 12, and 24 h after paxilline treatment (10, 20, and 40 μg/mL). $^{*}P < 0.05$ and $^{**}P < 0.01$ compared to the control.

Discussion

Hepatocellular carcinoma (HCC) is a progressive disorder that is increasing in prevalence and has a high mortality rate. The prognosis for HCC patients is poor because of the high rates of recurrence and metastasis of HCC[14]. Therefore, potent drugs need to be developed for treating HCC. Several researchers have suggested that plant-based products offer effective alternative strategies for treating tumors[15–18]. In this study, we showed that paxilline, a compound extracted from an endophytic fungus of *B. cusia*, promoted the apoptosis of HepG2 cells via autophagy.

'Pathways in cancer', a term of KEGG database, is related to cell proliferation, migration, apoptosis, and the cell cycle[19]. The results of the network pharmacology analysis revealed that 'pathways in cancer' was the most important signaling pathway involved in the anti-HCC effects of paxilline, which indicated that paxilline might regulate hepatocellular proliferation, migration, apoptosis, and the cell cycle. The protein mTOR is a key target for initiating autophagy, and the protein EGFR is a key target for regulating apoptosis. Both are key proteins that mediate the PI3K-AKT signaling pathway, with autophagy promoting apoptosis. We used the MCODE algorithm for further analysis and found that mTOR and EGFR were crucial targets and that the PI3K-AKT pathway was another important signaling pathway[20,21]. Further analysis of the molecular docking data revealed

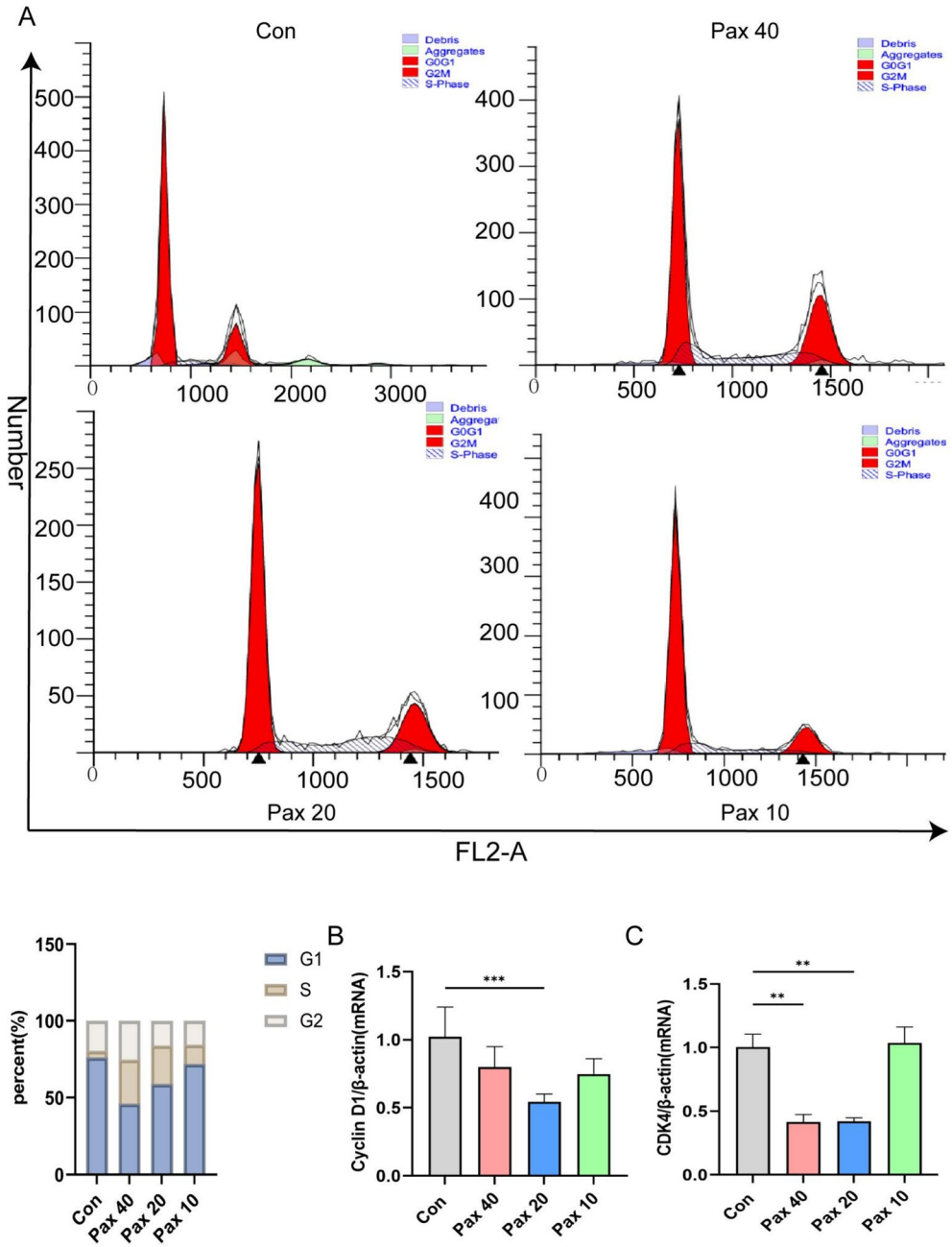

Fig. 5. Paxilline arrested HepG2 cells in the S phase. (**A**) Cell cycle distribution of paxilline-treated HepG2 cells after 48 h was determined by flow cytometry. (**B**, **C**) RT-qPCR of paxilline-treated HepG2 cells for 24 h at the mRNA level of cell cycle-related genes. *$P < 0.05$ and **$P < 0.01$ compared to the control.

that paxilline can effectively bind to apoptosis-related and autophagy-related proteins, with the best binding to the PIK3CA (gene name of PI3K) and mTOR. Thus, the results of the network pharmacology analysis revealed that the anti-HCC effect of paxilline might be related to apoptosis mediated by the autophagy signaling pathway. To further validate this results, we conducted in vitro experiments. The results of the CCK8 and wound-healing assays revealed that paxilline effectively repressed the proliferation and migration of HepG2 cells. The cell cycle is the process through which cells divide. Inducing cell cycle arrest may be a strategy for treating cancer[16]. The Cyclin D1-CDK4 complex is the crucial determinant that promotes the progression of the cell cycle from the G1 phase to the S phase[22]. We found that paxilline blocked HepG2 cells in the S phase by downregulating the expression of Cyclin D1 and CDK4. These results indicated that paxilline can induce HepG2 cell apoptosis by blocking the S phase.

The bcl-2 family is an important family of proteins that regulate apoptosis, including proapoptotic and antiapoptotic proteins. These proteins coordinate with each other during apoptosis and jointly determine whether a cell enters apoptosis by mediating the signaling pathway[23]. Caspase-3 acts as a promoter of apoptosis

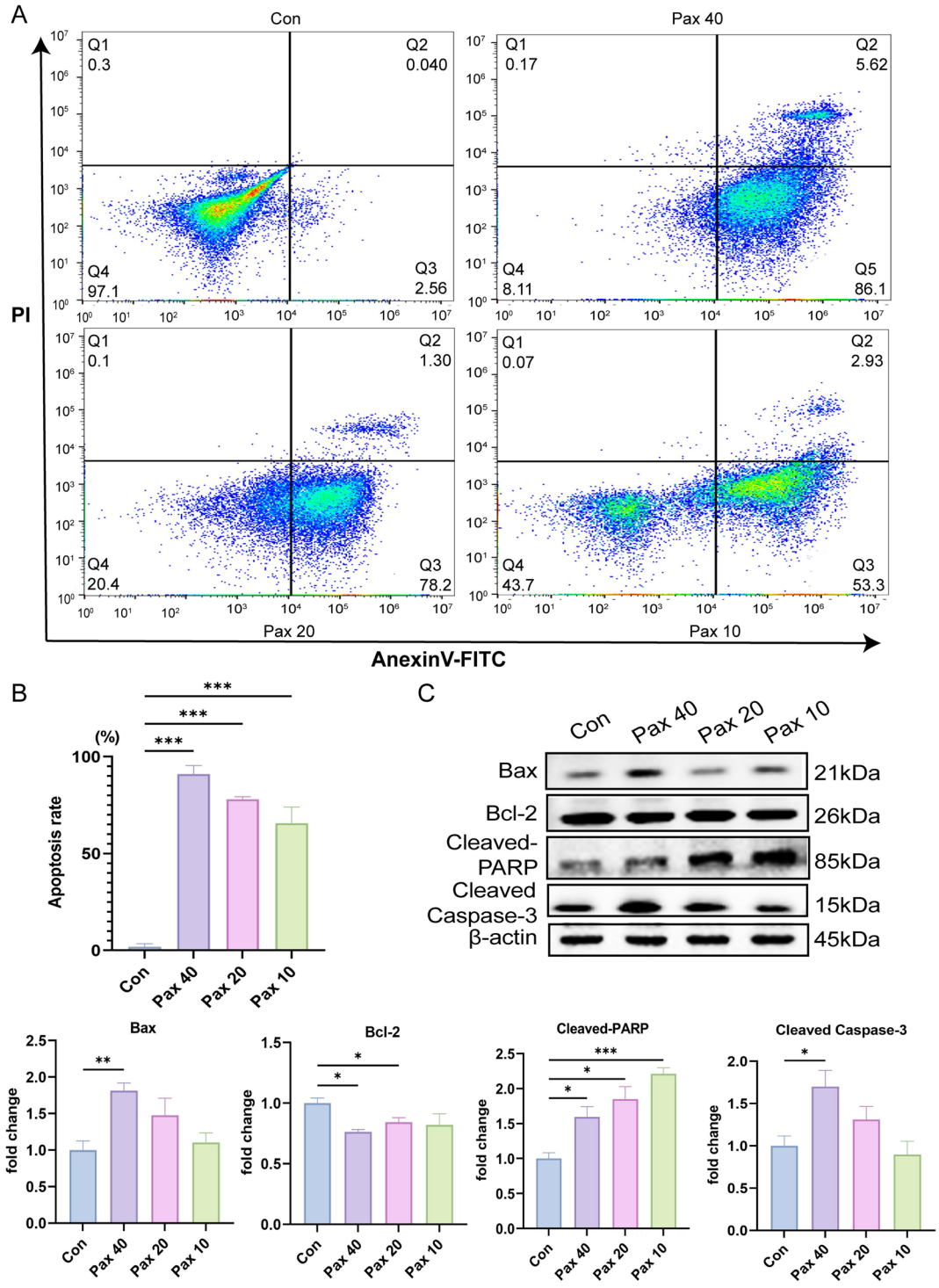

Fig. 6. Paxilline promoted apoptosis in HepG2 cells. (**A**, **B**) Effects of treatment with different concentrations of paxilline (10, 20, and 40 μg/mL) for 24 h on the percentage of apoptotic HepG2 cells. (**C**) Effects of treatment with different concentrations of paxilline (10, 20, and 40 μg/mL) for 12 h on the levels of apoptosis-related proteins. $^{*}P < 0.05$ and $^{**}P < 0.01$ compared to the control.

and shears the substrate poly ADP-ribose polymerase (PARP), which inhibits DNA repair[24]. Moreover, autophagy regulates the bcl family to promote apoptosis. We found that paxilline upregulated the expression of bax, cleaved-PARP, and cleaved caspase-3. Meanwhile, paxilline downregulated the expression of bcl-2. These results indicated that paxilline can induce HepG2 cell apoptosis by initiating the bcl-2 family.

Autophagy is a dynamic protective mechanism underlying the intracellular degradation of macromolecules and organelles to maintain cellular homeostasis. This process mainly involves macroautophagy and

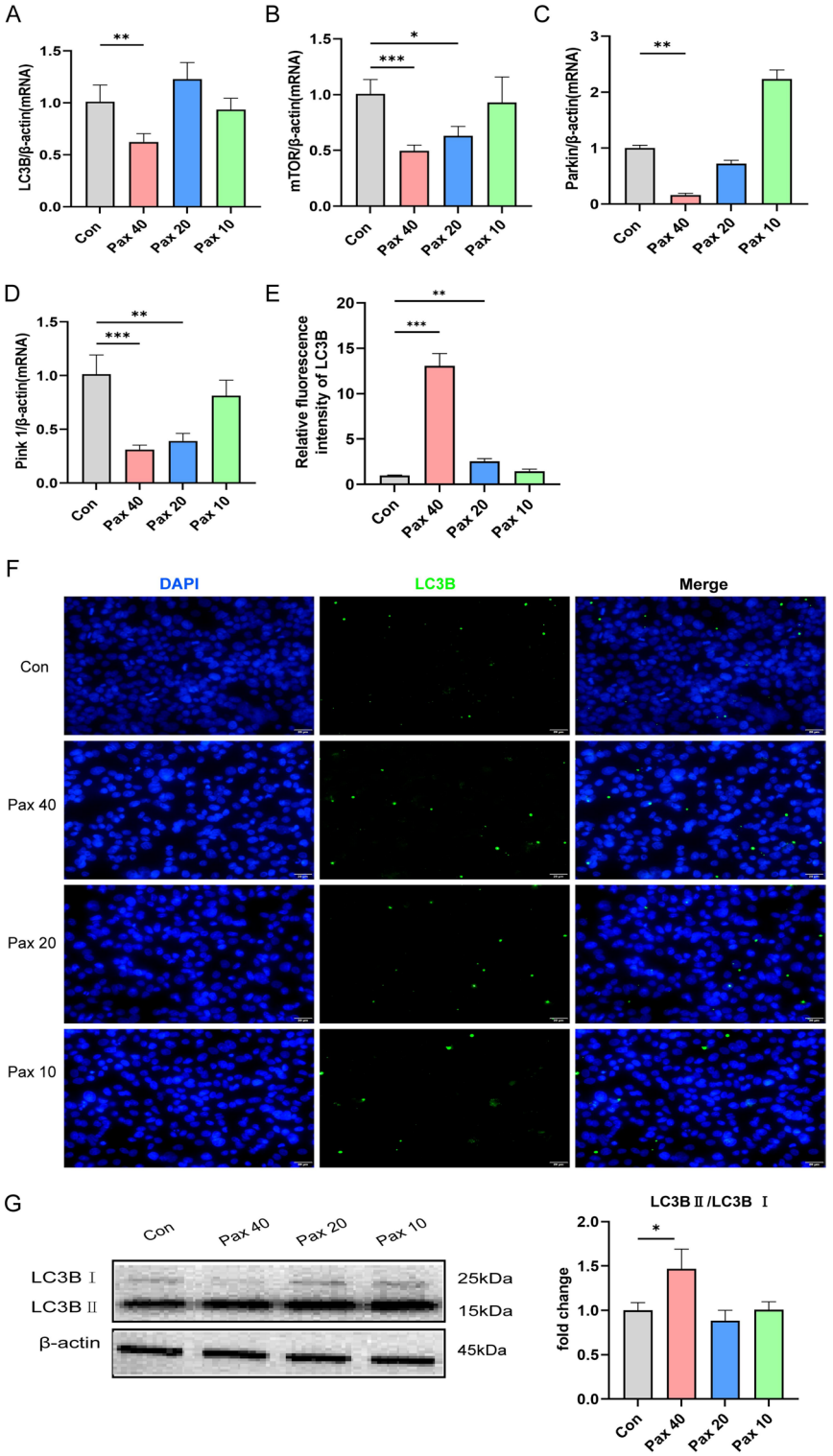

Fig. 7. Paxilline regulates autophagy in HepG2 cells. (**A**–**D**) The mRNA levels of autophagy-related genes in HepG2 cells exposed to different concentrations of paxilline (10, 20, and 40 μg/mL) for 24 h, as determined by RT-qPCR. (**E**, **F**) Paxilline inhibited the expression of LC3B in HepG2 cells for 24 h, as shown by immunocytochemistry; scale bar = 20 μm. **G** Protein levels of LC3B in HepG2 cells exposed to different concentrations of paxilline (10, 20, and 40 μg/mL) for 24 h, as determined by Western blotting analysis. $^{*}P < 0.05$ and $^{**}P < 0.01$ compared to the control.

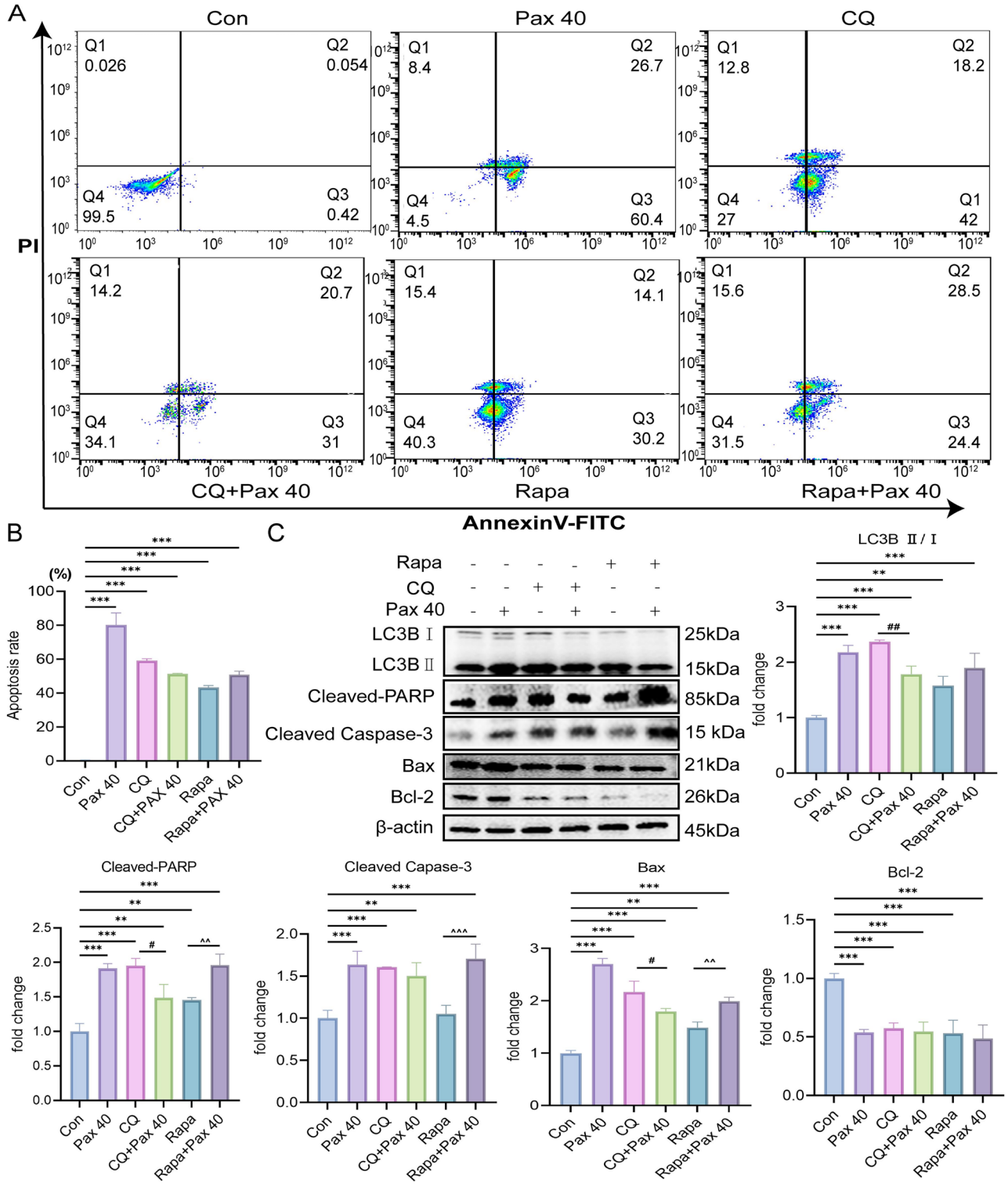

Fig. 8. Paxilline promoted apoptosis by mediating autophagy in HepG2 cells. (**A**, **B**) Annexin V-FITC analyses of the apoptotic rates of HepG2 cells exposed to paxilline (40 μg/mL) with or without CQ (10 μM)/Rapa (100 nM) for 24 h. (**C**) The expression of LC3B, Bax, Bcl-2, cleaved-caspase 3, and cleaved-PARP in HepG2 cells exposed to paxilline (40 μg/mL) with or without CQ (10 μM)/Rapa (100 nM) for 24 h. $^{*}P<0.05$ and $^{**}P<0.01$ compared to the control; $^{\#}P<0.05$ and $^{\#\#}P<0.01$ compared to the CQ group; $^{\wedge}P<0.05$ and $^{\wedge\wedge}P<0.01$ compared to the Rapa group.

microautophagy, with the main difference between the two types of autophagy being the presence or absence of autophagosome formation[25]. The results of this study revealed that paxilline significantly inhibited the expression of mTOR, which matched the results of the preexisting network pharmacology predictions. Moreover, mTOR initiates macroautophagy. LC3B, downstream of mTOR, is involved in autophagosome formation during macroautophagy[26]. We found that paxilline (40 μg/mL) significantly inhibited the mRNA expression of LC3B but significantly increased the level of the LC3B protein, possibly related to the post-translational modifications of proteins. Furthermore, the expression of LC3B II/I significantly increased, which indicated that paxilline promotes the formation of autophagosomes in macroautophagy[27,28]. Thus, these results showed that the anti-HCC effect of paxilline might be related to the regulation of the mTOR gene to promote autophagosome formation for initiating macroautophagy. However, the regulation of microautophagy by paxilline was not clear; therefore, we examined the microautophagy-related genes Pink1 and Parkin. The pink1/parkin signaling pathway is an important pathway to regulate microautophagy, which is closely related to mitochondrial autophagy[29,30]. In the presence of external stimuli, pink1 in mitochondria first phosphorylates itself and then recruits parkin in the cytoplasm; together they initiate mitochondrial autophagy. When pink1 or parkin was knocked down, neither of them could cause mitochondrial autophagy[31]. We found that paxilline significantly inhibited the mRNA expression of Pink1 and Parkin, suggesting that paxilline may regulate microautophagy.

We also verified our hypothesis by administering paxilline with CQ or Rapa in combination. In acidic lysosomes, CQ increases the lysosomal pH, inhibiting the fusion and degradation of autophagic lysosomes in cells, which results in the aggregation of LC3BII[32]. Rapa is an autophagy agonist that inhibits mTOR[33]. The results of this study revealed that challenge with CQ/Rapa alone or in combination with paxilline significantly promoted apoptosis and the expression of LC3BII/I, suggesting that the balance of autophagy was disrupted after treatment with CQ or Rapa and that the number of autophagosomes increased simultaneously. Paxilline significantly inhibited mTOR via a mechanism similar to that underlying the action of Rapa. We hypothesized that paxilline might promote autophagy and our results confirmed that. the expression of proapoptotic proteins was higher in the CQ group than in the CQ + paxilline group. The expression of proapoptotic proteins was higher in the Rapa + paxilline group than in the Rapa group. The expression of antiapoptotic proteins was significantly downregulated by CQ/Rapa alone or in combination with paxilline. To summarize, the anti-HCC effect of paxilline may be related to its ability to promote autophagy. However, this study had a limitation. We have only made a preliminary exploration of autophagy-mediated apoptosis, and we have not elucidated what kind of autophagy and autophagic lysosomes are specifically initiated by paxilline in HepG2 cells. In the future, we aim to conduct more in-depth studies to further elucidate the role of paxilline in the fight against hepatocellular carcinoma.

Conclusion

To summarize, network pharmacology and molecular docking analyses revealed that the mechanism underlying the anti-HCC effects of paxilline might be related to apoptosis and autophagy. In vitro experiments revealed that paxilline regulates apoptosis by mediating autophagy in HepG2 cells. This study provided preclinical evidence for the efficacy of paxilline in treating HCC and new insights into the treatment of HCC.

Data availability

The data supporting the findings of this study are included in this published article. Raw data generated and/or analysed during the current study are available from Yin Yuan, upon reasonable request.

Received: 3 December 2024; Accepted: 19 May 2025
Published online: 27 May 2025

References

1. Forner, A., Reig, M. & Bruix, J. Hepatocellular carcinoma. *Lancet* **391**, 1301–1314 (2018).
2. Bruix, J., Boix, L., Sala, M. & Llovet, J. M. Focus on hepatocellular carcinoma. *Cancer Cell* **5**, 215–219 (2004).
3. Vogel, A., Meyer, T., Sapisochin, G., Salem, R. & Saborowski, A. Hepatocellular carcinoma. *Lancet* **400**, 1345–1362 (2022).
4. Yang, C. et al. Evolving therapeutic landscape of advanced hepatocellular carcinoma. *Nat. Rev. Gastroenterol. Hepatol.* **20**, 203–222 (2023).
5. Zeng, M. et al. Expression and functional study of BcWRKY1 in *Baphicacanthus cusia* (Nees) Bremek. *Front. Plant Sci.* **13**, 919071 (2022).
6. Zhang, Q. et al. Psoriasis treatment using Indigo Naturalis: Progress and strategy. *J. Ethnopharmacol.* **297**, 115522 (2022).
7. Yu, J. et al. 7-methoxy-13-dehydroxypaxilline: New indole diterpenoid from an endophytic fungus Penicillium sp. Nb 19. *Nat. Prod. Res.* **38**, 103–111 (2024).
8. Duan, Y. et al. Role of autophagy on cancer immune escape. *Cell Commun. Signal.* **19**, 91 (2021).
9. Jiang, T., Chen, X., Ren, X., Yang, J. M. & Cheng, Y. Emerging role of autophagy in anti-tumor immunity: Implications for the modulation of immunotherapy resistance. *Drug Resist. Updates* **56**, 100752 (2021).
10. Emdad, L. et al. Recent insights into apoptosis and toxic autophagy: The roles of MDA-7/IL-24, a multidimensional anti-cancer therapeutic. *Semin. Cancer Biol.* **66**, 140–154 (2020).
11. Takamura, A. et al. Autophagy-deficient mice develop multiple liver tumors. *Genes Dev.* **25**, 795–800 (2011).
12. Tian, Y. et al. Autophagy inhibits oxidative stress and tumor suppressors to exert its dual effect on hepatocarcinogenesis. *Cell Death Differ.* **22**, 1025–1034 (2015).
13. Guo, X. L. et al. Targeting autophagy potentiates chemotherapy-induced apoptosis and proliferation inhibition in hepatocarcinoma cells. *Cancer Lett.* **320**, 171–179 (2012).
14. Yang, J. D. et al. A global view of hepatocellular carcinoma: Trends, risk, prevention and management. *Nat. Rev. Gastroenterol. Hepatol.* **16**, 589–604 (2019).
15. Li, J. K. et al. Gracillin exerts anti-melanoma effects in vitro and in vivo: Role of DNA damage, apoptosis and autophagy. *Phytomedicine* **108**, 154526 (2023).

16. Song, H. S., Jang, S. & Kang, S. C. Bavachalcone from Cullen corylifolium induces apoptosis and autophagy in HepG2 cells. *Phytomedicine* **40**, 37–47 (2018).
17. Fan, L. et al. Euphorbia factor L2 inhibits TGF-beta-induced cell growth and migration of hepatocellular carcinoma through AKT/STAT3. *Phytomedicine* **62**, 152931 (2019).
18. Gao, S. et al. Rabdosia rubescens (Hemsl.) H. Hara: A potent anti-tumor herbal remedy—Botany, phytochemistry, and clinical applications and insights. *J. Ethnopharmacol.* **340**, 119200 (2024).
19. Kanehisa, M. & Goto, S. KEGG: Kyoto encyclopedia of genes and genomes. *Nucleic Acids Res.* **28**, 27–30 (2000).
20. Li, R., Zheng, Y., Zhang, J., Zhou, Y. & Fan, X. Gomisin N attenuated cerebral ischemia-reperfusion injury through inhibition of autophagy by activating the PI3K/AKT/mTOR pathway. *Phytomedicine* **110**, 154644 (2023).
21. Novoplansky, O. et al. Activation of the EGFR/PI3K/AKT pathway limits the efficacy of trametinib treatment in head and neck cancer. *Mol. Oncol.* **17**, 2618–2636 (2023).
22. OuYang, F. et al. AKT signalling and mitochondrial pathways are involved in mushroom polysaccharide-induced apoptosis and G1 or S phase arrest in human hepatoma cells. *Food Chem.* **138**, 2130–2139 (2013).
23. Siveen, K. S. et al. Targeting the STAT3 signaling pathway in cancer: Role of synthetic and natural inhibitors. *Biochim. Biophys. Acta* **1845**, 136–154 (2014).
24. Zhou, J. et al. Targeting gastrin-releasing peptide receptors on small cell lung cancer cells with a bispecific molecule that activates polyclonal T lymphocytes. *Clin. Cancer Res.* **12**, 2224–2231 (2006).
25. Marsh, T. & Debnath, J. Autophagy suppresses breast cancer metastasis by degrading NBR1. *Autophagy* **16**, 1164–1165 (2020).
26. Yu, L. et al. Termination of autophagy and reformation of lysosomes regulated by mTOR. *Nature* **465**, 942–946 (2010).
27. Mikhaylova, O. et al. VHL-regulated MiR-204 suppresses tumor growth through inhibition of LC3B-mediated autophagy in renal clear cell carcinoma. *Cancer Cell* **21**, 532–546 (2012).
28. Devis-Jauregui, L., Eritja, N., Davis, M. L., Matias-Guiu, X. & Llobet-Navas, D. Autophagy in the physiological endometrium and cancer. *Autophagy* **17**, 1077–1095 (2021).
29. Nguyen, T. N. et al. Unconventional initiation of PINK1/Parkin mitophagy by Optineurin. *Mol. Cell* **83**, 1693-1709.e9 (2023).
30. Sorice, M. Crosstalk of autophagy and apoptosis. *Cells* **11**, 1479 (2022).
31. Nguyen, T. N., Padman, B. S. & Lazarou, M. Deciphering the molecular signals of PINK1/Parkin mitophagy. *Trends Cell Biol.* **26**, 733–744 (2016).
32. Lei, Y. et al. HBx induces hepatocellular carcinogenesis through ARRB1-mediated autophagy to drive the G(1)/S cycle. *Autophagy* **17**, 4423–4441 (2021).
33. Han, X. et al. Small molecule-driven NLRP3 inflammation inhibition via interplay between ubiquitination and autophagy: Implications for Parkinson disease. *Autophagy* **15**, 1860–1881 (2019).

Acknowledgements
Not applicable.

Author contributions
Y.Y., J.Y., and Y.L. conceived the experimental design, determined of methodology, and edited the manuscript; M.L., T.Z., Z.D., and C.Y. participated in the extraction of paxilline and network analysis; X.S, D.T, and Y.L. participated in charting, statistical analysis and results visualization. All authors reviewed the manuscript.

Funding
This work was supported by the Yunnan Science and Technology Talents and Platform Program (202205AF150071), Yunnan Fundamental Research Projects (grant NO. 202401AU070034), and Yunnan Province Innovation Guidance and Technology oriented Enterprise Cultivation Plan (No. 202404BI090001).

Declarations

Competing interests
The authors declare no competing interests.

Additional information
Supplementary Information The online version contains supplementary material available at https://doi.org/10.1038/s41598-025-03044-1.

Correspondence and requests for materials should be addressed to Y.L.